NO reduction with NH$_3$ under oxidizing atmosphere on copper loaded hydroxyapatite

Jihène Jemal[a], Hassib Tounsi[a,*], Kamel Chaari[b], Carolina Petitto[c], Gérard Delahay[c], Samir Djemel[a], Abdelhamid Ghorbel[a]

[a] Laboratoire de Chimie de Matériaux et Catalyse, Département de Chimie, Faculté des Sciences de Tunis, Campus Universitaires 1060 Tunis, Tunisia
[b] Laboratoire de Chimie Industrielle, Ecole Nationale d'Ingénieurs de Sfax, ENIS- BP 1173 – 3038 Sfax, Tunisia
[c] Institut Charles Gerhardt, UMR 5253 CNRS/UM2/ENSCM/UM1; Equipe "Matériaux Avancés pour la Catalyse et la Santé" Ecole Nationale Supérieure de Chimie de Montpellier, 8 rue de l'Ecole Normale, 34296 Montpellier Cedex, France

ABSTRACT

Copper loaded hydroxyapatite catalysts were prepared by ion exchange in aqueous phase. The copper ion exchange capacity of hydroxyapatite host structure is highly dependent on the initial copper concentration of the solution. For the lowest concentration, a pH variation of the exchange solution is observed. This change in pH may allow the deposition of a small amount of copper hydroxide at the expense of cationic substitution of copper. The increase in copper content exchanged has no effect on the profile of conversion of NO by NH$_3$. From this, it is assumed that the copper cations substituted for calcium are not active in the reaction. The profiles of NO conversion obtained, are in agreement with the presence of a small amount of copper oxide clusters deposited on the surfaces of the apatite.

© 2011 Elsevier B.V. All rights reserved.

1. Introduction

Nitrogen oxides (NO$_x$: x = 1, 2) issued from stationary and mobile sources remain a major source of air pollution. They contribute to acid rain, ozone depletion, ground-level ozone and green house effects [1,2]. With more and more stringent regulations concerning NO$_x$ emissions [3], the developing of an active and stable catalyst for NOx reduction in oxygen-rich atmosphere is an urgent task [4]. Unfortunately, the traditional three-way catalysts are effective for gasoline-powered engines, but cannot be used for diesel vehicles, because of the oxygen-rich atmosphere where NOx reduction cannot be achieved easily. Several technologies have been proposed to the abatement of NOx present in oxygen-rich exhaust gases issued from diesel and lean-burn gasoline engines [1,2]. The selective catalytic reduction with ammonia (NH$_3$-SCR) is considered as an effective post-treatment for NO$_x$ emission. For obvious reasons it would not be desirable to use NH$_3$ for automotive applications since it is corrosive, toxic and difficult to handle [4]. To overcome the difficulties associated with NH$_3$, urea was used as ammonia vector agent because it is safer and can generate NH$_3$ in situ by hydrolysis

[5]. NH$_3$/urea SCR technology has been adapted to heavy-duty (HD) and light-duty (LD) diesel vehicles with high NOx reduction efficiency [6]. Many catalysts have been reported to be active for NH$_3$-SCR in oxidizing atmosphere. The most widely employed catalysts are based on V$_2$O$_5$–WO$_3$ (MoO$_3$) supported titania [2]. Although vanadium catalyst has been introduced for HD diesel vehicles in Europe [7] since 2005, this material has some serious problems to overcome related to toxicity of vanadia species, the high activity for oxidation of SO$_2$ to SO$_3$ and to the rapid decrease in activity and selectivity above 500 °C. The drawbacks of vanadia catalysts shifted the research interest towards other catalytic systems. Among the new catalysts for mobile applications, copper and iron exchanged zeolites (MOR, BEA, and ZSM-5) have been found to be suitable for SCR applications at higher temperatures ($T > 400$ °C) [8–13]. Special attention is devoted to Fe-ZSM-5 [8,10–12] catalyst due to its high activity, high resistance to SO$_2$ and H$_2$O under SCR reaction conditions but its NO conversion at low temperature (<250 °C) is still poor. To improve the low temperature conversion, manganese-based catalysts such as Mn–Al$_2$O$_3$, Mn–TiO$_2$ and Mn–Cu mixed oxides have been reported active however they are not very stable and their resistance to H$_2$O and SO$_2$ should be enhanced [14,15].

In our previous work [16], we reported for the first time the excellent catalytic properties of copper loaded hydroxyapatite (Cu-HAp) catalysts over a broad temperature range in NH$_3$-SCR of NO

in oxygen rich atmosphere. It was found that the highly dispersed CuO particles on Ca-Hap surfaces were responsible for the NO conversion in the low temperature range. The increase of exchange time induced an increase of the size of CuO clusters that became less active in NH_3-SCR. This study was devoted to the preparation of highly dispersed CuO particles on Ca-Hap by controlling the exchange conditions (copper concentration and exchange time). The prepared catalysts were tested in the NH_3-SCR of NO under oxidizing atmosphere and characterized with XRD, N_2 sorption, UV–vis and H_2-TPR techniques.

2. Experimental

2.1. Preparation of support and catalysts

The hydroxyapatite (Ca-Hap) powder was prepared by an aqueous precipitation method using $(NH_4)_2HPO_4$ and $Ca(NO_3)_2 \cdot 4H_2O$ as starting materials and ammonia solution for pH adjustment [17]. Two series of Cu-Hap catalysts were prepared at room temperature (RT) by introducing 1.5 g of Ca-Hap into 50 cm^3 of copper nitrate solution under magnetic stirring and with measuring initial (pH_i) and final pH (pH_f). The pH_f values were those measured after interaction of Ca-Hap with the solution of known pH_i. For the first series, 0.15 M copper nitrate solution was used and the exchange time has been varied: 15, 30, 60, 120, and 1440 min, respectively. The second series of Cu-Hap catalysts was obtained by varying the concentration of copper nitrate in the exchange solution: 0.01, 0.025, 0.05, 0.10 and 0.15 M with an exchange time of 15 min. The solids recovered after filtration were washed with water, dried at 70 °C for 7 h and finally calcined at 500 °C in air during 2 h.

2.2. Characterization techniques

The calcium content was estimated by direct complexometric titration with EDTA at pH > 12. The phosphorus was determined by absorption photometry after formation of the yellow phosphatomolybdic complex (λ_{max} = 460 nm) using UV-Spectrophotometer SP-3000 plus OPTIMA. The copper amount was obtained from chemical analysis by atomic absorption spectroscopy with Analytik Jena ZEEnit 700.

The pH of point of zero charge ($pHpzc$) of the support Ca-Hap was assessed according to the following protocol. Samples masses of 1 g were contacted with 20 mL of distilled water. The slurry was sonicated during 3 min and then magnetically stirred for 24 h at RT. Initial pH (pH_i) values were set in the range of 3–11, by adding minimum amounts of NaOH or HCl. After equilibration, pH values were measured once again (pH_f). The pHpzc was determined as the point where the pH_f vs. pH_i curve crosses the line $pH_i = pH_f$.

The crystallinity of the catalysts was established by Philips Powder X-ray diffractometer DATA-MP SIEMENS D 501 using Cu Kα (λ = 0.15418 nm) incident radiation equipped with a Si detector.

The nature of the Cu species was determined by UV–visible spectroscopy. Diffuse reflectance spectra were recorded in the UV–vis region (200–900 nm) with Jasco V-570 spectrometer equipped with an integrating sphere for solid samples and using $BaSO_4$ as reference.

The textural properties of the samples were determined by adsorption and desorption of N_2 at 77 K, using Micromeritics ASAP 2020. The BET method was used to determine the specific area whereas the pore size and volume were estimated using the Barret–Joyner–Halenda (BJH) approximation.

The nature, reducibility and amount of Cu species were estimated by temperature programmed reduction with hydrogen (H_2-TPR). The experiments were carried out with a Micromeritics 2910 apparatus using H_2/Ar (3/97, v/v) gas at a total flow-rate
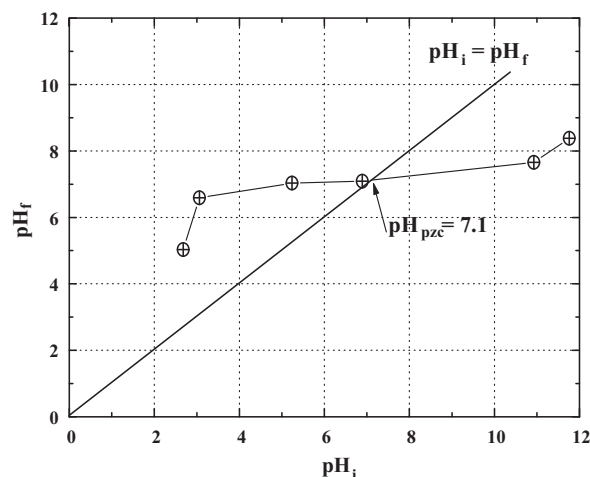

Fig. 1. pH_{pzc} of Ca-Hap determined as the point where the pH_f vs. pH_i curve crosses the line $pH_i = pH_f$.

of 15 cm^3 min^{-1} and by heating the samples from RT to 1000 °C (10 °C min^{-1}). In each case, 0.051 g of the catalyst was previously activated at 550 °C for 30 min under air, and then cooled to RT under the same gas. The TPR with H_2/Ar (3/97, v/v) was then started and the thermal conductivity detector monitored continuously H_2 consumption.

The NH_3-SCR of NO was studied in catalytic microflow reactor operating at atmospheric pressure. An aliquot of the catalyst (0.022 g) was activated in situ at 550 °C for 1 h under a flow of O_2/He (20/80, v/v) and then cooled to RT. A feed mixture of 400 ppm NO, 400 ppm NH_3 and 8% O_2 in He was then was then passed through the catalyst at a flow rate of 100 cm^3 min^{-1}. The NO-SCR was carried out on programmed temperature from 100 °C to 500 °C with the heating rate at 6 °C min^{-1}. The reactants and products were analyzed by a quadruple mass spectrometer (Pfeiffer Omnistar) equipped with Channeltron and Faraday detectors (0–200 amu) following these characteristic masses: NO (30), N_2 (14, 28), N_2O (28, 30, 44), NH_3 (17, 18), O_2 (16, 32) and H_2O (17, 18).

3. Results and discussion

3.1. Copper ion exchange study

The chemical analysis, of the Ca-Hap host structure, shows a calcium deficient with a Ca/P close to 1.55 (Ca wt.% = 38.40 and P = 19.16). Chemical analysis of copper of Cu-Hap catalysts, prepared from the same large excess of copper in solution is reported in Table 1. The pH_i of copper solutions suggested that the dominant species are Cu^{2+} ions [19]. The initial concentration of copper nitrate has a great effect on the copper quantity introduced. For the lowest copper concentrations, due to Ca-Hap buffer properties, an increase of the pH_f was noted. This can be explained on the basis of proton-competitive sorption reactions without precipitation of copper hydroxide species at the surface of the host structure. It can be said that H^+ ions compete with Cu^{2+} ions for the surface sites of Ca-Hap. The pH_f observed for the exchange with 0.01 M as initial concentration is similar to that obtained with Ca-Hap alone (Fig. 1). This figure reports the pH_{pzc} of Ca-Hap determined as the point where the pH_f vs. pH_i curve crosses the line $pH_i = pH_f$. A value of pH_{pzc} = 7.1 was assessed for our Ca-Hap which is in agreement with the results reported in Ref. [18]. It is well known that Ca-Hap has excellent buffering properties in the absence of specific sorption of copper from the solution [21–23]. In the range of pH values below pH_{pzc} = 7.1; consumption of protons from the solution by the protonation of surface $\equiv PO^-$ and $\equiv CaOH^0$ groups results in a final

Table 1
Preparation conditions of Cu-Hap catalysts, chemical analysis of copper, S_{BET} area and pore diameter.
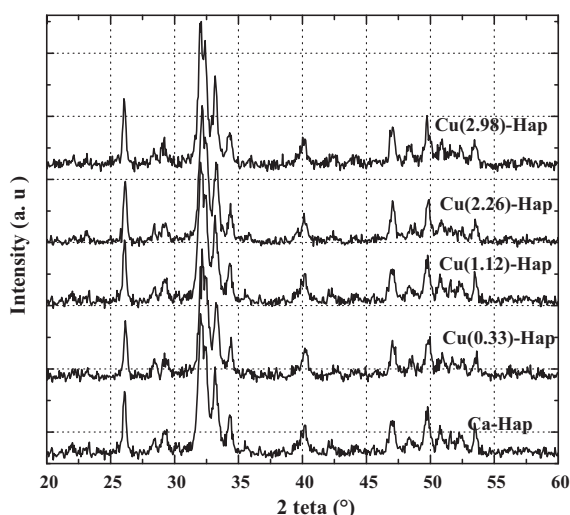
Catalysts	$[Cu^{2+}]$ (M)	Exchange time (min)	pH_i	pH_f	Cu (wt.%)	S_{BET} (m^2/g)	Pore diameter (nm)
Ca-Hap	–	–			0	35	18
Cu(0.36)-Hap	0.01	15	5.2	7.2	0.36	–	–
Cu(0.33)-Hap	0.025	15	4.9	6.3	0.33	27	25
Cu(0.37)-Hap	0.05	15	4.7	5.3	0.37	–	–
Cu(1.12)-Hap	0.10	15	4.5	5.0	1.12	34	17
Cu(2.44)-Hap	0.15	15	4.0	4.1	2.44	–	–
Cu(2.52)-Hap	0.15	30	–	–	2.52	–	–
Cu(2.26)-Hap	0.15	60	–	–	2.26	33	22
Cu(2.61)-Hap	0.15	120	–	–	2.61	–	–
Cu(2.98)-Hap	0.15	1440	–	–	2.98	32	28

pH increase. The positively charged ≡CaOH$_2$$^+$ and neutral ≡POH^0 sites prevail on Ca-Hap surface in acidic solutions, making surface charge positive at pH values below pH_{pzc} [22]. This feature was clearly observed for the lowest copper concentration where the pH evolves from 5.2 to 7.2, which is close to pH_{pzc}. A copper concentration of 0.10 M improves the quantity introduced but the best result is reached with an initial concentration of 0.15 M.

On the other hand, the influence of exchange time was investigated in the range of 15–1440 min at a Cu^{2+} concentration of 0.15 M which gives the best results without significant pH variation. On the basis of chemical analysis, the exchange of Cu^{2+} on Ca-Hap from solution was very fast and was completed within a matter of minutes. After an exchange time of 15 min the amount of copper reaches a value of 2.44 wt.%. Despite the increase of contact time to 1440 h, there is a slight increase of the amount of copper and a value of 2.98 wt.% was reached. This result suggested that Ca-Hap and aqueous cupric ions displayed two distinct modes of interaction [19,20]. The first was a very rapid ion exchange occurring in a few minutes followed by a slower increase of copper species occurring over a period of many days. The rapid interaction suggests that the exposed Ca^{2+} ions were immediately exchanged with Cu^{2+} ions which become chermisorbed onto the surface. The slower increase of the amount of cation sorbed is due to gradual occupancy of active sites and decreasing Cu^{2+} concentration in the liquid phase.

3.2. X-ray powder diffraction (XRD) analysis

X-ray diffraction patterns of Ca-Hap powder and the prepared Cu-Hap catalysts were reported in Fig. 2. The observed positions of diffraction lines are in full agreement with the corresponding values reported for hexagonal Ca-Hap (PDF Ref. 09-0432) [24]. The

Ca-Hap structure was not altered by copper ion exchange whatever the exchange time and copper concentration.

The knowledge of the exact locations of copper ions in the Ca-Hap structure is very important to understand the active sites for the NH$_3$-SCR of NO. It is well known that Ca-Hap, with unit cell formula Ca$_{10}$(PO$_4$)$_6$(OH)$_2$, crystallizes in the hexagonal $P6_3/m$ space group. The structure can be described as a quasi compact assemblage of tetrahedral of [PO$_4$]$^{3-}$ in which delimit two types of zeolite-like channels. The first type of channel has an average diameter of about 2.5 Å and contains 4 Ca^{2+} ions, noted Ca(I), surrounded by nine oxygen atoms. The second type has an average diameter of 3.5 Å contains 6 Ca^{2+} ions, noted Ca(II), surrounded by seven oxygen atoms, one of which belongs to the OH$^-$ groups and the others to the PO$_4$$^{3-}$ tetrahedral. The structure of Ca-Hap allows different substitutions and ion exchanges. The Ca^{2+} ions can be partially replaced by bivalent cations (Pb^{2+}, Cu^{2+}, Zn^{2+}, Fe^{2+}, Ba^{2+}, etc.) and perhaps also by trivalent species [25].

Misra et al. [26] suggested on the basis of crystallographic consideration that Cu^{2+} ions exchange with the three easily accessible Ca ions (two on the surface and one beneath that is associated with water molecules) on the exposed face (1 0 0) of Ca-Hap. On the other hand, Corami et al. [27] concluded from structure simulation and EXAFS experiments that Ca(II) sites could be more suitable to host Cu^{2+} and the adsorption of Cu^{2+} happens in the surface sites substituting H$^+$ or Ca^{2+}. The migration in the inner part of the structure is unlikely due to the considerable difference in radii of the two exchanging ionic species; 0.099 and 0.072 nm for Ca^{2+} and Cu^{2+}, respectively.

In our case, we think that Cu(H$_2$O)$_6$$^{2+}$ exchanged on Ca-Hap retains its inner sphere structure, without hydrolysis, due to the low pH_i used for the preparation of catalysts. The further air-calcination at 500 °C for 2 h leads to the formation of dehydrated Cu^{2+} ions and fine particle of copper oxide dispersed on the surface of Ca-Hap.

3.3. Nitrogen adsorption–desorption

In Table 1, were reported the BET surface area (S_{BET}) and BJH desorption average pore diameter of the prepared catalysts. Concerning textural properties, it was shown in previous work that Ca-Hap and Cu-Hap catalysts have typical type IV suggesting that the solids are mostly mesoporous [16]. Moreover, the introduction of copper to Ca-Hap does not change significantly S_{BET} and the pore diameter.

3.4. Diffuse reflectance UV–vis spectroscopy

Fig. 3 shows the diffuse reflectance UV–visible spectra of Ca-Hap and the Cu-Hap samples. Ca-Hap shows a band at 205 nm assigned to O^{2-} → Ca^{2+} charge transfer [28]. On the other hand, copper exchanged catalysts show an intensive absorbance band centred at 256 nm which can be assigned to low energy charge transfer (LCT) O^{2-} → Cu^{2+} of copper ions in tetrahedral coordination

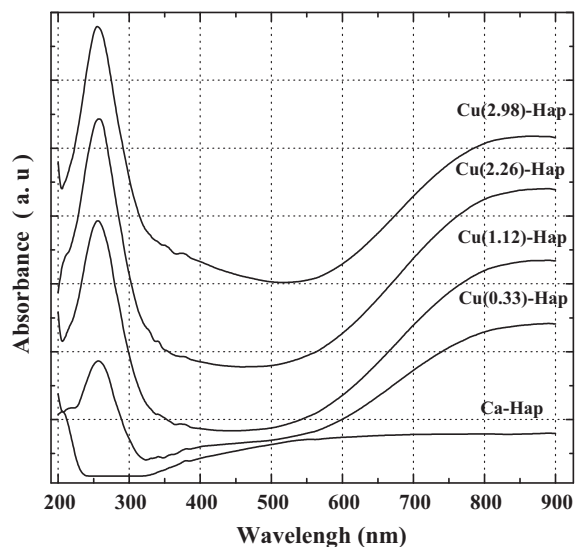**Fig. 2.** XRD patterns of the Ca-Hap support and Cu-Hap catalysts.

Fig. 3. UV–vis spectra of Ca-Hap and Cu-Hap catalysts.

[29,30]. In addition, a broad peak in the 550–900 nm range corresponds to d–d transitions of Cu^{2+} in tetrahedral coordination surrounding by oxygen in CuO. The increase of the baseline between 375 and 600 nm for Cu(2.98)Hap can be related to d–d transition of Cu^{2+} ions in libethenite $Cu_2(OH)PO_4$ crystals formed by dissolution/precipitation mechanism on the surface of Ca-Hap crystals [16].

3.5. Temperature-programmed reduction (TPR) analysis

The H_2-TPR profiles of pure Hap and Cu-Hap catalysts are reported in Fig. 4. In Table 2 were reported the temperatures at which the reduction rate is maximal (T_m) for low temperature (LT) and for high temperature (HT) peaks and H_2/Cu ratios. As shown in our previous work [16], Ca-Hap profiles show three reduction peaks related to the reduction of phosphates species at temperatures ($T > 450\,°C$), which can interfered with the reduction of copper species. For Cu-Hap catalysts, the reduction profiles can be divided into low LT region ($T < 300\,°C$) and HT region ($300 < T(°C) < 550$). The LT reduction profiles contain mainly one peak with shoulders and can be attributed to the reduction of fine particles of CuO to Cu^0
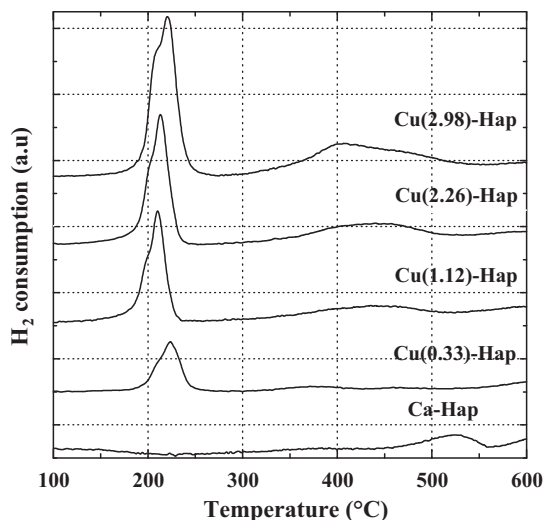

Fig. 4. H_2-TPR profiles of Ca-Hap and Cu(x)Hap catalysts. Conditions: H_2/Ar (3/97, v/v), flow rate = 30 cm³ min⁻¹, ramp: 10 °C min⁻¹, catalyst mass = 0.051 g.
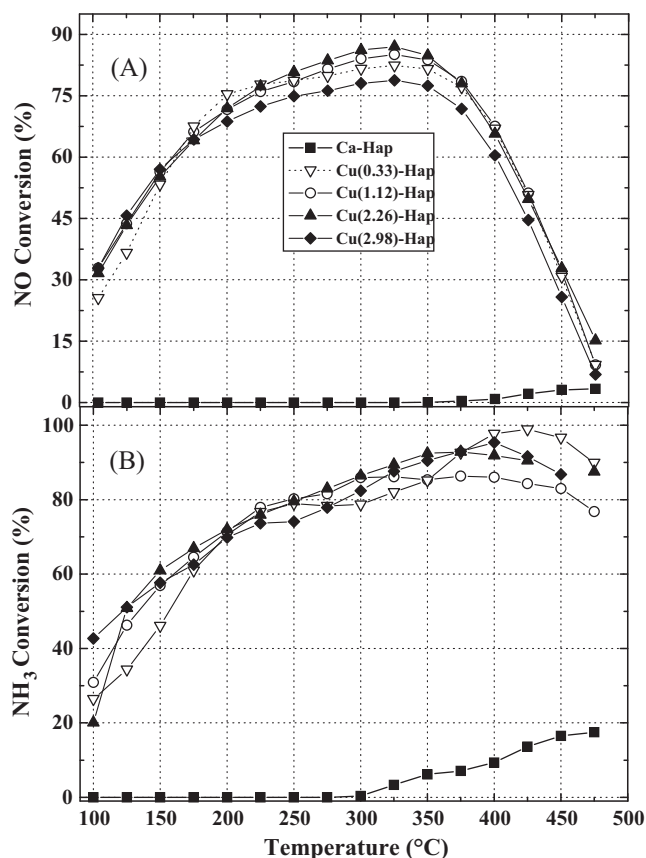

Fig. 5. SCR of NO by NH_3 of the studied catalysts. (A) NO conversion; (B) NH_3 conversion. TPSR protocol: ramp = 6 °C min⁻¹, flow rate = 100 cm³ min⁻¹, catalyst mass = 0.022 g, [NO] = [NH_3] = 400 ppm, [O_2] = 8% balanced with He.

with different size and eventually small quantity of Cu^{2+} to Cu^+. The presence of isolated Cu^{2+} cations in Cu-Hap cannot be excluded. The broad HT peaks at around 400 °C, which is ascribed to the reduction of Cu^+ to Cu^0; formed from the reduction of Cu^{2+} at LT; confirm the presence of isolated Cu^{2+}. From the increase of copper amount it results, as expected, the increase of the intensity of LT and HT TPR peaks of Cu-Hap. For Cu(2.98)-Hap, besides the reduction of Cu^+ to Cu^0, the HT peak can be attributed to the reduction of Cu^{2+} cations in the new solid phase-libethenite $Cu_2(OH)(PO_4)$ formed by dissolution/precipitation mechanism on the surface of Ca-Hap crystals. The quantitative analysis shows H_2/Cu molar ratios close to unity which corresponds to the stoichiometric reduction of Cu^{2+} to Cu^0 (Table 2). The high ratio of H_2/Cu observed for Cu(0.33)Hap is probably due to the low copper content of this sample by taking into account that an hydrogen consumption was observed for Ca-Hap.

3.6. Selective catalytic reduction of NO by NH_3

Fig. 5 shows the NO and NH_3 conversion profiles over Ca-Hap and Cu-Hap catalysts and the maximum NO conversions and the related temperatures were reported in Table 3. The reduction of NO by NH_3 in presence of an excess of O_2 proceeds according to the following Eq (1):

$$4NO + 4NH_3 + O_2 \rightarrow 4N_2 + 6H_2O \tag{1}$$
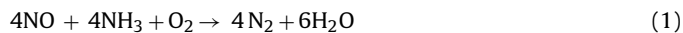
which is known as the standard reaction.

The introduction of a small amount of copper to Ca-Hap, which is inactive for NO reduction, produces marked changes in the catalytic behavior. As seen for Cu(0.33)-Hap catalyst, NO conversion

Table 2
The temperatures at which the reduction rate is maximal (T_m) and H_2/Cu ratios.

Catalyst	LT peak T_m (°C)	HT peak		Total H_2/Cu (mol/mol)
		T_m (°C)	Surface (%)	
Cu(0.33)-Hap	208 (sh[a]); 224	375	15	1.79
Cu(1.12)-Hap	197 (sh); 210	440	33	1.18
Cu(2.26)-Hap	200 (sh); 214	435	46	0.99
Cu(2.98)-Hap	208 (sh); 220	406	49	1.16

[a] sh: shoulder.

Table 3
The maxima of NO conversions obtained (with the related temperatures) of the different Cu-Hap catalysts.

Catalyst	Max of NO conversion (%)	T_{max} (°C)
Cu(0.33)Hap	83	336
Cu(1.12)Hap	85	326
Cu(2.26)Hap	87	321
Cu(2.98)Hap	79	310

started around 100 °C (27%), reached 83% at 336 °C with a negligible production of N_2O (2 ppm) and then decreased progressively to 10% at 475 °C. With the increase of copper content there was only a slight increase of NO conversion in the medium temperature range of 250–350 °C, excepted for Cu(2.98)-Hap where a slight decrease is observed. On the other hand, Cu-Hap catalysts exhibited NH_3 conversion very close to NO conversion until its maximum then continues to grow up above it. This behavior reveals a competition between reduction of NO by NH_3 and NH_3 oxidation into NO or/and N_2O. Surprisingly, the best efficient catalyst was Cu-Hap with the lowest copper content. It can be suggested that highly dispersed CuO clusters that are easily reduced were responsible for the NO conversion in the low temperature range for Cu(0.33)Hap catalyst. The increase of copper solution concentration leads to an increase of the amount of this active species which slightly enhanced the NO conversion at medium temperature range of 250–350 °C. On the other hand, it can be concluded that the exchange time is a determinant factor for the preparation of active copper species. The best exchange time should be chosen with respect of the rapid interaction mode of Ca-Hap and aqueous cupric ions. This rapid interaction is related to the exchange of Cu^{2+} cations for the easiest accessible Ca(II) sites at the Ca-Hap surface. The increase of the exchange time leads the formation of inactive copper species by a dissolution-precipitation process that occurs from the copper

adsorbed on the surface of Ca-Hap. This result is clearly shown in Fig. 6 in which we reported the NO conversion of Cu(1.12)Hap and two others catalysts, from Ref. [16], having the same copper content but different exchange time. For example, at 150 °C, the NO conversion of Cu(1.12)Hap catalyst (exchange time 15 min) is about 56%, which decreases to 43% after 6 h (Cu(6)Hap) of exchange and drops to 27% after 30 h (Cu(30)Hap).

4. Conclusions

Recently we have shown that high loading copper hydroxyapatite are much less active catalysts in the NH_3-SCR of NOx than copper exchange Ca-Hap containing 1% Cu due to the formation of libethenite phase. In this new study, one of the goals was also to prepare high loading copper Ca-Hap catalyst by avoiding this inactive phase. This objective was reached since no XRD peaks of the libethenite phase were observed for Cu-Hap prepared by ion exchange and containing copper content above 2.5 wt.% Cu.

Although the maximum exchange capacity of copper is not reached for the prepared catalysts, it was not observed, as for the Cu–zeolite systems, an increase in the conversion of NO with the copper content. On the contrary, the most loaded copper catalyst has a slightly lower conversion above 180 °C. Thus, all the samples efficiently operated in the low temperature region, while, at higher temperatures, oxidation of ammonia by oxygen significantly decreased the NO conversion. It is generally assumed that isolated Cu^{2+} cations catalyse the reaction at higher temperature, while oligomers or bulky copper oxide species are active in the region of low temperatures. UV–vis and TPR results suggest the presence of isolated Cu^{2+} cations in our samples but in tetragonal sites, which we suppose to be not active for the reaction. Therefore, dispersed CuO clusters found at low copper content are supposed to be responsible for the NO conversion of the catalysts. Of course considering the weak specific surface of the materials, it is obvious that probably a large amount of the copper species introduced in the Ca-Hap is not accessible. The increase of the activity of this class of materials in the reaction must be realised by developing the surface area. One of the possibilities is to attempt a deposition on an adequate support. Our current research on these materials has focused on this objective.

Fig. 6. SCR of NO by NH_3 of Cu(1.12)Hap (this study) and Cu(6)Hap, Cu(30)Hap (from Ref. [16]) catalyst. TPSR protocol: ramp = 6 °C min^{-1}, flow rate = 100 cm^3 min^{-1}, catalyst mass = 0.022 g, [NO] = [NH_3] = 400 ppm, [O_2] = 8% balanced with He.

References

[1] K. Skalska, J.S. Miller, S. Ledakowicz, Sci. Total Environ. 408 (2010) 3976–3989.
[2] S. Roy, M.S. Hegde, G. Madras, Appl. Energy 86 (2009) 2283–2297.
[3] Dieselnet, 2011. http://www.dieselnet.com.
[4] Z. Liu, S.I. Woo, Catal. Rev. 48 (2006) 43–89.
[5] F. Birkhold, U. Meingast, P. Wassermann, O. Deutschmann, SAE Technical Paper (2006) 2006-01-0643.
[6] T.V. Johnson, SAE Technical paper (2009) 2009-01-0121.
[7] E. Jacob, R. Muller, A. Schneeder, T. Cartus, R. Dreisbach, H. Mai, M. Paulus, J. Spengler, Hochleistungs-SCR-katalysatorsystem: garantie fur niedrigste NOx emission. Motortechnische Zeitschrift, vol. 67, 2006.
[8] S. Brandenberger, O. Kröcher, A. Tissler, R. Althoff, Catal. Rev. 50 (2008) 492–531.
[9] G. Carja, G. Delahay, C. Signorile, B. Coq, Chem. Commun. (2004) 1404–1405.
[10] M. Colombo, I. Nova, E. Tronconi, Catal. Today 151 (2010) 223–230.
[11] G. Qi, Y. Wang, R.T. Yang, Catal. Lett. 121 (2008) 111–117.

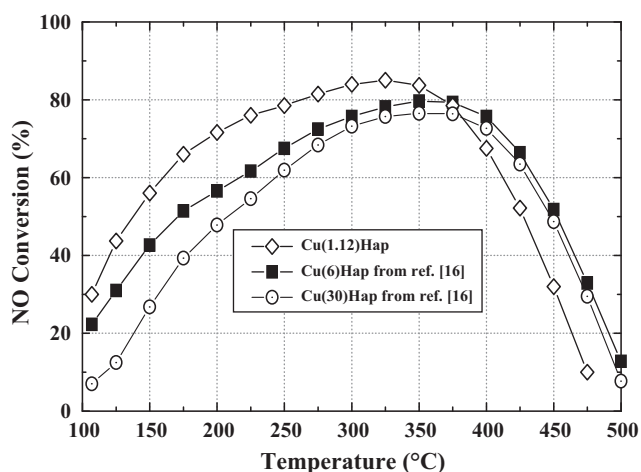[12] W. Arous, H. Tounsi, S. Djemel, A. Ghorbel, G. Delahay, Catal. Commun. 6 (2005) 281–285.

[13] P. Markatou, J. Dai, A. Johansson, W. Klink, M. Castagnola, T.C. Watling, SAE Technical Paper (2011) 2011-01-1304.

[14] R. Jin, Y. Liu, Z. Wu, H. Wang, T. Gu, Chemosphere 78 (2010) 1160–1166.

[15] J. Li, H. Chang, L. Ma, J. Hao, R.T. Yang, Catal. Today (2011), doi:10.1016/j.cattod.2011.03.034.

[16] H. Tounsi, S. Djemel, C. Petitto, G. Delahay, Appl. Catal., B 107 (2011) 158–163.

[17] J.C. Heughebaert, PhD Thesis, Institut National Polytechnique Toulouse, 1977.

[18] M. Kosmulski, J. Colloid Interface Sci. 353 (2011) 1–15.

[19] M. Sljivic, I. Smiciklas, I. Plecas, M. Mitric, Chem. Eng. J. 148 (2009) 80–88.

[20] S. Bruckner, G. Lusvardi, L. Menabue, M. Saladini, J. Mater. Chem. 3 (1993) 715–719.

[21] I.D. Smiciklas, S.K. Milonjic, P. Pfendt, S. Raicevic, Sep. Purif. Technol. 18 (2000) 185–194.

[22] L. Wu, W. Forsling, P.W. Schindler, J. Colloid Interface Sci. 147 (1991) 178–185.

[23] M.F. Elkady, M.M. Mahmoud, H.M. Abd-El-Rahman, J. Non-Cryst. Solids 357 (2011) 1118–1129.

[24] International Centre for Diffraction Data, Powder Diffraction File, 09-0432.

[25] J.C. Elliot, Structure, Chemistry of the Apatites and Other Calcium Orthophosphates, Elsevier, Amsterdam, 1994.

[26] D.N. Misra, R.L. Bowen, B.M. Wallace, J. Colloid Interface Sci. 51 (1) (1975) 36–43.

[27] A. Corami, F. D'Acapito, S. Mignardi, V. Ferrini, Mater. Sci. Eng. B 149 (2008) 209–213.

[28] P. Rulis, L. Ouyang, W.Y. Ching, Phys. Rev. B 70 (2004) 155104–155111.

[29] R.A. Schoonheydt, Catal. Rev. Sci. Eng. 35 (1993) 129–168.

[30] H. Praliaud, S. Mikhailenko, Z. Chajar, M. Primet, Appl. Catal., B 16 (1998) 359–374.